Published in final edited form as:
*Acad Radiol*. 2008 February ; 15(2): 260–264.

# Hyperpolarized $^{3}$He MR imaging of the lung: Effect of subject immobilization on the occurrence of ventilation defects

**Jaime Mata**[1], **Talissa Altes**[1,3], **Jeffrey Knake**[1], **John Mugler III**[1,2], **James Brookeman**[1,2], and **Eduard de Lange**[1]

1 *Center for In-vivo Hyperpolarized Gas MR Imaging, Department of Radiology, University of Virginia School of Medicine, Charlottesville, Virginia, USA*

2 *Department of Biomedical Engineering, University of Virginia School of Medicine, Charlottesville, Virginia, USA*

3 *Department of Radiology, Children's Hospital of Philadelphia, Philadelphia, Pennsylvania, USA*

## Abstract

**Purpose—**To investigate immobilization-induced ventilation defects when performing hyperpolarized $^{3}$He ($H^{3}He$) MRI of the lung.

**Methods and Materials—**Twelve healthy subjects underwent MRI of the lungs following inhalation of $H^{3}He$ gas at three time points: 1) immediately after having been positioned supine on the MR scanner table, 2) at 45 minutes while remaining supine, 3) and immediately thereafter after having turned prone. All image sets were reviewed in random order by three independent, blinded readers who recorded number, location and size of $H^{3}He$ ventilation defects. Scores were averaged for each time point and comparisons were made to determine change in number, location and size of ventilation defects with time and positioning of the subject in the scanner.

**Results—**At baseline supine there were small numbers of defects in the dependent (posterior) and non-dependent (anterior) portions of the lung ($p=0.625$). At 45 minutes there was a significant increase in the mean number of ventilation defects/slice (VDS) for the dependent ($p=0.005$) and a decrease for the non-dependent lung portions ($p=0.021$). After subjects turned prone, mean VDS for posterior defects decreased significantly ($p=0.011$) while those for anterior defects increased ($p=0.010$). Most defects were less than 3 cm in diameter.

**Conclusion—**It was found that immobilization of the subject for an extended period of time led to increased number of $H^{3}He$ ventilation defects in the dependent portions of the lung. Therefore, after a subject is positioned in the scanner, $H^{3}He$ MR imaging should be performed quickly to avoid the occurrence of the immobilization-induced ventilation defects, and possible overestimation of disease.

### Keywords

lung; atelectasis; hyperpolarized helium; MR imaging; ventilation defects

Corresponding author: Jaime Mata, Ph.D., Dept. of Radiology, Box 801339, University of Virginia, Charlottesville, VA, 22908, USA, Phone: 434-243-6498, Fax: 434-924-9435, Email: jfm4q@virginia.edu.

## Introduction

Hyperpolarized helium-3 ($H^3He$) is a gaseous magnetic resonance (MR) imaging contrast agent that, when inhaled, can be used to evaluate the airspaces of the lung. With this technique high-spatial-resolution MR images of lung ventilation can be obtained as has been shown in numerous studies involving normal volunteers and patients with a variety of diseases (1–5, 24,25). Although there is generally homogeneous distribution of the MR signal throughout the lung in healthy subjects following inhalation of the gas, small peripheral ventilation defects in the dependent areas of the lungs can been seen and are believed to be caused by collapse of small portions of the lung (3,5). The purpose of this study was to investigate the effect of patient positioning and time on the frequency, size and location of these defects, in order to better understand their impact and significance in the diagnosis of pulmonary disease when using $H^3He$ MR. Our findings were compared with earlier work done in posture-dependence of lung function, in animal studies and patients, using a variety of other modalities (7–10,12–14,18, 19).

## Materials and Methods

### Subjects

The study group consisted of 12 healthy, volunteers who had never smoked (six men and six women; age range, 22–43 years; median age, 34 years) and had no history of lung disease. None of them had undergone $H^3He$ MR imaging of the lungs previously. All volunteers had to meet the following criteria: normal physical examination, normal spirometric results [predicted forced expiratory volume in one second ($FEV_1$) of 80% or greater; ratio of $FEV_1$ to Forced Vital Capacity ($FEV_1$/FVC) greater than 0.70], normal chest radiography, greater than 95% oxygen saturation at pulse oximetry and no known allergies. All studies were performed with approval from the Food and Drug Administration for using $H^3He$ as an Investigational New Drug (IND # 57,866) and under a protocol approved by our institution's Investigational Review Board. All volunteers provided informed written consent prior to their studies.

### $^3He$ Polarization

The $^3He$ gas was polarized using a commercial system (model IGI 9600, MITI, Durham, NC) via the spin exchange method using rubidium vapor as the alkali metal in the process. The rubidium vapor was optically pumped with a 60-Watt diode array laser (wavelength centered at 795nm). The details of the polarization process have been described in detail previously (1). After polarizing the gas for approximately 17 hours, achieving polarization levels ranging from 30–38%, the gas was cooled down for 45 minutes. For each set of $^3He$ MR images to be obtained, approximately 350 ml of $H^3He$ was passed through a polytetrafluoroethylene (PTFE) membrane filter (0.003 μm poresize, Millipore, Japan) and dispensed into a Tedlar® bag (Jensen Inert Products, Coral Springs, FL). Medical grade nitrogen was added to the bag to provide a total volume of one liter. The bag with gas was then transported to the scanner and inhaled by the subject.

### MR Imaging

All studies were performed by using a 1.5 Tesla whole-body MR scanner (Magnetom Vision, Siemens Medical Solutions, Malvern, PA), modified with a broadband amplifier to allow operation at the $^3He$ resonant frequency of 48 MHz. A specially designed flexible radio-frequency coil (IGC Medical Advances, Milwaukee, WI) tuned to the $^3He$ frequency was wrapped around the volunteer's chest during the entire study. Throughout the imaging, the subject's heart rate and blood oxygen saturation were monitored (Omni-track Vital Signs Monitoring System, Invivo Research, Orlando, FL). The mean oxygen saturation value at the

end of each breath-hold was 94 ± 2.2%. Two minutes after the breath-hold, all subjects had completely recovered and showed values identical to their baselines (98 ± 0.9%).

For each volunteer, a single set of axial $H^3He$ MR images was obtained after the subject had been positioned in supine position on the table of the MR scanner with the flexible radio-frequency coil around the chest. Including the time for scout images and slice positioning, the set of $H^3He$ images was typically obtained within five minutes that the subject was on the table. After the scan, the subject remained supine on the scanner table within the flexible coil but with the table moved out of the scanner for subject comfort. While on the table the subject was asked to breath normally. After 40 minutes the scanner table with the subject supine was moved back into the scanner and a second set of axial $H^3He$ images was obtained, which was typically about 45 minutes after the initial scan. Following the second scan, the patient table was again moved out of the scanner, the radio-frequency coil was loosened, and the volunteer was asked to turn to the prone position. Subsequently, after adjusting the radio-frequency coil, the scanner table was moved back into the scanner and a third set of axial $H^3He$ images obtained with the subject prone.

Each image set consisted of 23–25 contiguous sections obtained by using a two-dimensional gradient-echo pulse sequence with following parameters: repetition time (TR)/echo time (TE) 7.0 ms/2.7 ms; flip angle 9°; matrix size 128×128; voxel size of 3.3 mm ×3.3 mm; section thickness, 10 mm. Each scan was performed during a breath-hold period of approximately 15 seconds immediately following inhalation of the $H^3He$ gas.

## Image Analysis

Three $H^3He$ MR image sets (baseline supine, 45-minute supine and prone) for all 12 subjects were printed separately on film whereby the prone images were rotated by 180 degrees to facilitate reviewing. Images were printed without any subject information or technical indicators except for the display of a ruler as provided by the standard software of the scanner. Subsequently, the image sets were distributed in random order to three radiologist readers. Each reader determined, independently and without information as to the order in which the images had been obtained, the number of $H^3He$ ventilation defects for each image section, the number of defects that were located in the anterior or posterior, superior or inferior, and right or left portion of the lung, and the number of defects that were <3 cm or >3 cm in maximum dimension. For determination of whether a defect was in the anterior or posterior half of the lung, the reviewers used the imaginary coronal plane through the trachea and main stem bronchi, and for the superior versus inferior half of the lung, the reviewers used the horizontal plane through the carina. A ventilation defect was defined as an area of the lung that completely lacked gas signal (appearing black) or a sharply defined area with diminished signal intensity (appearing less bright than the surrounding lung).

## Statistical Analysis

For each image set the scores from the three reviewers were averaged and the mean number of ventilation defects per slice (individual subject VDS) computed for each of the 3 image sets of the individual subjects. Subsequently, the mean VDS for the group of 12 subjects was calculated at each time point for the whole lung, anterior versus posterior half, superior versus inferior half, right versus left, and for defects < 3 cm and > 3 cm. The statistical significance of differences was assessed by using a two-tailed paired t-test, with a p-value $<0.05$ being considered statistically significant.

## Results

The mean VDS for the 12 healthy volunteers at baseline supine, 45-minute supine and prone are presented in Table 1. At baseline, small numbers of defects were seen (individual subject VDS range 0.15 – 3.03; mean, 0.87 ± 0.89), with no significant differences in mean VDS for the group of 12 subjects between the dependent (posterior) and non-dependent (anterior) portions of the lung (p=0.625). After remaining supine for 45 minutes, there was an overall increase (p=0.035) in VDS (individual subject range: 0.25 – 3.21; mean, 1.43 ± 0.96). This increase was largely due to a more than two-fold increase in mean VDS for the group in the dependent portion of the lung (p=0.005) while there was a significant decrease in mean VDS in the non-dependent portion (p=0.021). When the subjects subsequently turned prone, mean VDS of posterior defects decreased again markedly (p=0.011) for the group of 12 subjects to values that were slightly but not significantly below baseline while there was a marked increase (p=0.010) in mean VDS of anterior defects to values that were slightly but not significantly above baseline, resulting in a decrease of the overall mean VDS for the whole lungs to a value that was slightly but not significantly above baseline (individual-subject VDS range with subject prone: 0.27–2.57; mean 1.00 ± 0.67).

There was a relatively greater change in mean VDS for the group in the left lung compared to that for the right lung, both with the subjects supine at 45 minutes and prone; however, the difference in mean VDS between the two lungs was not statistically significant at any of the three time points. Similarly, at all three time points, the mean VDS involving the inferior half of the lung was always slightly, but not significantly greater than that for the superior half (Table 1).

With respect to defect size, the defects were mostly small (<3 cm) at baseline. With the increase of defects at 45 minutes, there was an almost two-fold increase in mean VDS for small (< 3cm) defects (p=0.130) while mean VDS for large (> 3cm) defects remained essentially unchanged (p=0.743). When the subjects turned prone, both the small and large defects decreased in number but stayed above baseline values for the small defects (p=0.490) and decreased to below baseline values for the large defects (p=0.060).

The three reviewers showed a very similar evaluation of the images, with an average standard deviation of 0.038 VDS among all images from baseline, and 0.049 and 0.045 VDS for the images obtained at 45 minutes and in prone position, respectively.

## Discussion

In this study in normal individuals we found that there was a significant increase in $H^3He$ ventilation defects in the posterior, dependent, portions of the lung after the subjects had been immobilized for a relatively long period of 45-minute period in the supine position. The number of posterior defects more than doubled compared to baseline. Clearly, these defects had developed in the interval that the subjects remained immobilized. In the anterior, non-dependent portions of the lungs the defects decreased slightly in number during immobilization. The defects that formed in the dependent aspect of the lung, were transitory in nature because immediately after the subjects turned prone most of these resolved and the values returned to near baseline. It was also found that a greater proportion of defects developed in the upper lung zones (the lung above the level of the carina) compared to the lower lung.

Although the cause of these transient defects is uncertain, a likely explanation is that these were caused by compression of the alveoli from the weight of the lung above it when the subject is supine. This would be supported by the fact that the defects occurred chiefly at the periphery, that is, the most dependent aspects of the lung, and there were less defects further away from the periphery. It seems understandable that the effect of compression becomes more prominent

when immobilization is maintained over a longer period of time. A similar postulation of the effect of gravitational forces on the alveolar tissues has been made in humans in the upright or standing position whereby the alveoli at the bases of the lung are more compressed than those in the apices, and studies have indeed shown that the pattern of stress distribution is greatest in the direction of the gravity (20,21). An anterior-posterior gradient in lung density has also been demonstrated in a variety of cross-sectional imaging studies with the subjects supine. For instance, using CT it has been shown that with expiration the tissue density of the posterior, gravity-dependent lung increases more rapidly than that of the anterior lung, implying that the posterior regions empty more rapidly than the anterior regions (22). The heart and abdomen also contribute to the greater compression of the posterior lung regions in the supine position (23). Gravitational-dependent atelectasis is a common finding in the dependent portions of the lung using computed tomography (8,12,14,17,18) and has been investigated in animal studies and patients using a variety of other modalities including $H^3He$ MR (7–10,12–14,18,19).

In our study we found few ventilation defects on the $H^3He$ MR images present at baseline in many of the healthy subjects. Most (80%) of these defects were small, measuring less than 3 cm in diameter. While there was an increase in defects number in the dependent portions of the lungs with prolonged immobilization, the majority (89%) of the defects remained small. It was also found that there was a trend toward more defects in the left than right lung during immobilization, although the differences were not significant. It is possible that the heart, which is positioned on the left, causes additional compression on the lung (7,13,15).

One of the limitations of our study is that our study population was small and that the subjects were healthy and young. Older subjects or patients with diseases that involve airway narrowing such as asthma may be more susceptible to the development of gravity dependent atelectasis. Further, pediatric subjects may also have an increased susceptibility due to the small airway diameter and increased airway compliance.

## Conclusion

Nevertheless, the findings show that prolonged immobilization can lead to a significant increase in the number of $H^3He$ ventilation defects in the gravity dependent portions of the lung. Although most of these defects are small (< 3cm diameter) and disappear when the subject changes position, there is the potential in patients with lung diseases such as asthma or emphysema, who are likely to have defects already at baseline, that the additional presence of the immobilization-induced defects may lead to an overestimation of disease. It is therefore important that $H^3He$ MR images are obtained without delay after the subject is positioned in the MR scanner to avoid the development of these induced, gravity-dependent ventilation defects and potential for overestimation of disease severity.

#### Acknowledgements

This work was supported in part by the National Institutes of Health grant RO1-HL066479, the Commonwealth of Virginia Technology Research Fund grant IN2002-01 and Siemens Medical Solutions.

We would like to thank John Christopher, RT(R)(MRI), Doris Harding, RN, and Joanne Gersbach, RN, CCRC, for their valuable assistance with the subjects.

## References

1. de Lange EE, Mugler JP, Brookeman JR, et al. Lung Air Spaces: MR Imaging Evaluation with hyperpolarized $^3He$ Gas. Radiology 1999;210:851–857. [PubMed: 10207491]
2. MacFall JR, Charles HC, Black RD, et al. Human lung air spaces: potential for MR imaging with hyperpolarized He- 3. Radiology 1996;200:553–558. [PubMed: 8685356]

3. Kauczor HU, Hofmann D, Kreitner KF, et al. Normal and abnormal pulmonary ventilation: visualization at hyperpolarized He-3 MR imaging. Radiology 1996;201:564–568. [PubMed: 8888259]
4. Donnelly LF, MacFall JR, McAdams HP, et al. Cystic Fibrosis: Combined Hyperpolarized $^{3}$He Enhanced and Conventional Proton MR Imaging in the Lung-Preliminary Observations. Radiology 1999;212:885–889. [PubMed: 10478261]
5. Altes TA, Powers PL, Knight-Scott J, et al. Hyperpolarized $^{3}$He MR lung ventilation imaging in asthmatics: Preliminary findings. JMRI 2001;13:378–84. [PubMed: 11241810]
6. Wright FW. Atelectasis or collapse? Do those who use the former imply a neonatal aetiology? British Journal of Radiology 2001;74:874–875. [PubMed: 11560839]
7. Nieto MJ, Barba GP, Mangado NG, et al. Similar ventilation distribution in normal subjects prone and supine during tidal breathing. J Appl Physiol 2002;92:622–626. [PubMed: 11796673]
8. Hedenstierna G. Atelectasis and gas exchange during anesthesia. Electromedica 2003;71(1):70–73.
9. Warner DO. Preventing Postoperative Pulmonary Complications. The Role of the Anesthesiologist Anesthesiology 2000;92(5):1467–1472.
10. West, J. Respiratory Physiology – The essentials. 7. Lippincott Williams & Wilkins; 2004. p. 104
11. Crawford A, Cotton D, Paiva M, Engel L. Effect of airway closure on ventilation distribution. J Appl Physiol 1989;66(6):2511–2515. [PubMed: 2745313]
12. Morimoto S, Takeuchi N, Imanaka H, et al. Gravity-Dependent Atelectasis Radiologic, Physiologic and Pathologic Correlation in Rabbits on High-Frequency Oscillation Ventilation. Invest Radiology 1989;24:522–530.
13. Raoof S, Chowdhrey N, Raoof S, et al. Clinical Investigations in Clinical care. Effect of Combined Kinetic Therapy and Percurssion Therapy on the Resolution of Atelectasis in Critically Ill Patients . Chest 1999;115(6):1658–1665. [PubMed: 10378565]
14. Tomiyama N, Takeuchi N, Imanaka H, et al. Mechanism of Gravity-dependent Atelectasis, Analysis by Nonradioactive Xenon-Enhanced Dynamic Computed Tomography. Investigative Radiology 1993;28(7):633–638. [PubMed: 8344814]
15. Marcucci C, Nyhan D, Simon B. Distribution of pulmonary ventilation using Xe-enhanced computed tomography in prone and supine dogs. J Appl Physiol 2001;90:421–430. [PubMed: 11160037]
16. Mullan BF, Galvin JR, Zabner J, Hoffman EA. Evaluation of in Vivo Total and Regional Air Content and Distribution in Primate Lungs with High-Resolution CT. Academic Radiology 1997;4:674–679. [PubMed: 9344289]
17. Herold CJ, Kuhlman JE, Zerhouni EA. Pulmonary Atelectasis: Signal Patterns with MR Imaging. Radiology 1991;178:715–720. [PubMed: 1994407]
18. Tusman G, Bohm S, Tempra A, Melkun F, Garcia E, Turchetto E, Mulder P, Lachmann B. Effects of Recruitment Maneuver on Atelectasis in Anesthetized Children. Anesthesiology 2003;98(1):14–22. [PubMed: 12502973]
19. Fichele S, Woodhouse N, Swift A, et al. MRI of Helium-3 Gas in Healthy Lungs: Posture Related Variations of Alveolar Size. JMRI 2004;20:331–335. [PubMed: 15269962]
20. West J. Distribution of mechanical stress in the lung, a possible factor in localization of pulmonary disease. Lanvcet 1971;1:839–841.
21. West J, Matthews F. Stresses, strains and surface pressure in the lung caused by its weight. J Appl Physiol 1972;32:332–345. [PubMed: 5010043]
22. Hoffman EA. Effect of body orientation on regional lung expansion: a computed tomographic approach. J Appl Physiol 1985;59:468–480. [PubMed: 4030599]
23. Margulies S, Rodarte J. Shape of the chest wall in the prone and supine anesthetized dog. J Appl Physiol 1990;68:1970–1978. [PubMed: 2361898]
24. van Beek EJ, Wild JM, Kauczor HU, Schreiber W, Mugler JP 3rd, de Lange EE. Functional MRI of the lung using hyperpolarized 3-helium gas. J Magn Reson Imaging 2004;20:540–54. [PubMed: 15390146]
25. de Lange EE, Altes TA, Patrie JT, Gaare JD, Knake JJ, Mugler JP, Platts-Mills TA. Evaluation of asthma with hyperpolarized helium-3 Magnetic Resonance Imaging: Correlation with Clinical Severity and Spirometry. CHEST 2006;130:1055–1062. [PubMed: 17035438]

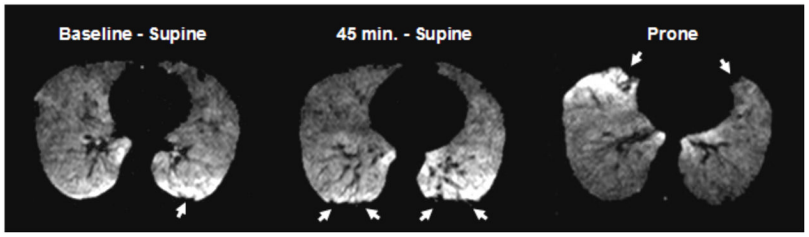


**Figure 1.**

Axial $H^3He$ MR images at the same level of a healthy subject at three different time points. (A) At baseline a small defect is seen posteriorly (arrow) in the dependent portion of the lung. (B) Image obtained 45 minutes after the subject has remained immobilized in supine position on the MR scanner shows marked interval increase in ventilation defects in the dependent portions of the lungs (arrows). (C) Image obtained immediately after the subject turned prone shows resolution of most posterior defects and development of new defects (arrows) in the newly dependent, anterior portion of the lung (image was rotated to facilitate comparison).

**TABLE 1**

Presentation of the mean number (± standard deviation) of $H^3He$ MR ventilation defects per slice (VDS) for the group of 12 subjects imaged at three time points: Baseline supine, 45-minute supine, and immediately after turning prone.

| | Baseline | p* | 45 min. | p* | Prone | p* |
|---|---|---|---|---|---|---|
| **Entire lung** | 0.87 ± 0.89 | | 1.43 ± 0.96 | | 1.00 ± 0.67 | |
| **Anterior**<br>**Posterior** | 0.40 ± 0.036<br>0.47 ± 0.072 | 0.625 | 0.24 ± 0.029<br>1.19 ± 0.161 | 0.007 | 0.59 ± 0.076<br>0.41 ± 0.048 | 0.058 |
| **Defects <3 cm**<br>**Defects >3 cm** | 0.69 ± 0.064<br>0.17 ± 0.015 | 0.012 | 1.28 ± 0.154<br>0.16 ± 0.016 | 0.034 | 0.92 ± 0.053<br>0.08 ± 0.008 | 0.001 |
| **Right Lung**<br>**Left Lung** | 0.43 ± 0.044<br>0.44 ± 0.067 | 0.893 | 0.66 ± 0.112<br>0.78 ± 0.145 | 0.428 | 0.56 ± 0.076<br>0.44 ± 0.049 | 0.227 |
| **Superior**<br>**Inferior** | 0.37 ± 0.037<br>0.50 ± 0.071 | 0.307 | 0.66 ± 0.123<br>0.77 ± 0.136 | 0.396 | 0.48 ± 0.062<br>0.53 ± 0.067 | 0.500 |

* Refers to the difference between the two values shown to the left of each p-value